



Short communication

## Binderless fabrication of amorphous RuO<sub>2</sub> electrode for electrochemical capacitor using spark plasma sintering technique

K. Kuratani, H. Tanaka, T. Takeuchi, N. Takeichi, T. Kiyobayashi\*, N. Kuriyama

Research Institute for Ubiquitous Energy Devices, National Institute of Advanced Industrial Science and Technology (AIST), 1-8-31 Midorigaoka, Ikeda, Osaka 563-8577, Japan

## ARTICLE INFO

## Article history:

Received 4 February 2009

Received in revised form 16 February 2009

Accepted 16 February 2009

Available online 3 March 2009

## Keywords:

Pseudocapacitor

Ruthenium oxide

Spark plasma sintering

Amorphous

Water content

## ABSTRACT

The spark plasma sintering (SPS) technique was successfully used to mold a hydrous amorphous RuO<sub>2</sub> electrode without any additives and binders. At the cyclic voltammetry (CV) scan rate of 1 mV s<sup>-1</sup>, the electrochemical capacitances of the RuO<sub>2</sub> electrodes are 600–700 F g<sup>-1</sup> for the entire electrode. An increase in the SPS current during the compaction led to the crystallization and dehydration of RuO<sub>2</sub>, which in turn, resulted in a significant decrease in its capacitance. There is room to improve the rate properties as we observed a steep drop in the capacitance when the CV scan rate was raised.

© 2009 Elsevier B.V. All rights reserved.

### 1. Introduction

In 1971, Trasatti et al. discovered that a RuO<sub>2</sub> film exhibited a featureless rectangular cyclic voltammogram, namely, a pseudocapacitive behavior [1]. Two decades later, Zheng et al. found that hydrous amorphous ruthenium oxide, RuO<sub>2</sub> · xH<sub>2</sub>O, possessed a capacitance of more than 700 F g<sup>-1</sup> [2,3]. Since then, conductive metal oxide pseudocapacitors [4–6] have been competing with electrochemical double-layer capacitors to meet the ever growing demand for high power density devices.

In many studies, the electrochemical capacitance is reported in terms of per mass of electrochemically active materials; that is, the mass of the non-capacitive additives is not included in calculating the gravimetric capacitance, and the ‘net’ capacitance is reported. In reality, not only for the ruthenium oxide, but also for other powdery materials in general, 5–10 wt% of a polymer binder (e.g., polyvinylidenedifluoride-*N*-methyl-2-pyrrolidone (PVdF-NMP)) is added to fix the powder in order to form an electrode. For the less electron-conductive powders, another 5–20 wt% of electron-conductive additives, e.g., acetylene black, is also mixed at the expense of the ‘gross’ gravimetric capacitance in which the total mass of electrode is taken into account. An interesting attempt to improve the gross capacitance of the RuO<sub>2</sub> electrode is to mix a more capacitive, but less conductive amorphous RuO<sub>2</sub> with a more

conductive, but less capacitive crystalline RuO<sub>2</sub> whereby the net capacitance reaches 982 F g<sup>-1</sup> [7]. Even in this case, however, a certain technique is required to fix the powder. On the one hand, reporting the net capacitance is significant to scientifically evaluate the intrinsic properties of the active materials under consideration. On the other hand, from the viewpoint of application, it is desirable to reduce the amount of the electrochemically inert additives in order to increase the gross capacitance and, probably, to reduce the production cost. One may think of a sintering method as an alternative to solidify a metal oxide powder without a binder. The problem of high temperature sintering is that, due to dehydration and crystallization, it is difficult to retain the amorphous and hydrous state (RuO<sub>2</sub> · xH<sub>2</sub>O) which is a requisite for the high capacitance [2]. (Hereafter, for simplicity, we denote ruthenium oxide as RuO<sub>2</sub> unless otherwise stated.)

The spark plasma sintering (SPS) technique [8,9] is effective for circumventing the crystallization and dehydration of RuO<sub>2</sub> because the intense, but short pulse of electric current passing through the powder under high pressure can compact the powder without affecting the bulk properties of the material. In this short communication, we report our preliminary results to prove the applicability of the SPS technique to fabricate a hydrous and amorphous RuO<sub>2</sub> electrode for use in an electrochemical capacitor.

### 2. Experimental

The RuO<sub>2</sub> powder was precipitated by the hydrolysis of RuCl<sub>3</sub> · nH<sub>2</sub>O (aq, 0.1 mol dm<sup>-3</sup>, 100 ml) by dropwise adding NaOH (aq, 0.3 mol dm<sup>-3</sup>, 100 ml). The obtained powder was washed with

\* Corresponding author. Tel.: +81 72 7519651; fax: +81 72 7519629.

E-mail address: [kiyobayashi-t@aist.go.jp](mailto:kiyobayashi-t@aist.go.jp) (T. Kiyobayashi).

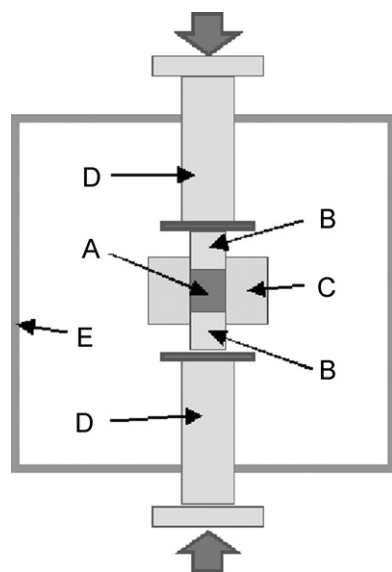


**Fig. 1.** Schematic drawing of the SPS apparatus: (A) sample powder, (B) WC punch, (C) Al<sub>2</sub>O<sub>3</sub> die, (D) electrode piston, and (E) closed chamber filled with N<sub>2</sub>.

distilled water, heated at 423 K for 17 h in air and sieved into a < 75 μm fraction.

SPS was performed using an SPS-515S (SPS Syntex). Fig. 1 shows a schematic illustration of the SPS apparatus. The RuO<sub>2</sub> powder (A) is loaded in conductive tungsten carbide punches (B) and an alumina insulator die (C) (10 mm φ), so that the electric current (SPS current) flows only through the RuO<sub>2</sub> powder. A uniaxial pressure and electric current are applied by the electrode pistons (D). The air in the chamber (E) is replaced by nitrogen before processing. In the present study, we varied the SPS current from 0 to 1 kA, fixing the mass of the RuO<sub>2</sub> powder to 250 mg, the compacting pressure to 50 MPa and the electrifying period to 1 s.

The crystallinity and morphology were examined using a powder X-ray diffractometer (XRD, Rigaku RINT2000, Cu Kα) and a scanning electron microscope (SEM, Hitachi S-5000). Thermal gravimetry and differential thermal analysis (TG–DTA, Rigaku Thermoplus TG 8120) were used to investigate the water content and the fraction of the amorphous component in the sample. The nitrogen adsorption and desorption isotherms at 77 K were measured using a Micromeritics ASAP 2010 to evaluate the surface area and porosity. For the material characterization mentioned above, the compacted RuO<sub>2</sub> sample by SPS was pulverized again into a powder in an agate mortar.

The cyclic voltammogram (CV) was measured in H<sub>2</sub>SO<sub>4</sub> (aq, 0.5 mol dm<sup>-3</sup>) using an ALS CHI 608B electrochemical analyzer with

the three-electrode setup in which a platinum mesh counter electrode and the standard calomel reference electrode (SCE) were used. The working electrode was prepared by wrapping the compacted RuO<sub>2</sub> disc with a gold mesh as the current collector ('SPS RuO<sub>2</sub>' hereafter). For comparison, we prepared two RuO<sub>2</sub> electrodes using the conventional method by mixing 90 or 95 wt% RuO<sub>2</sub> powder and 10 or 5 wt% PVdF–NMP as the binder (RuO<sub>2</sub>/10% PVdF and RuO<sub>2</sub>/5% PVdF, respectively). In both cases, the obtained slurry mixture was spread onto a Ti foil followed by drying at 383 K under vacuum to form the working electrode.

### 3. Results and discussion

Under a pressure of 50 MPa, the SPS current of more than 50 A was necessary to form a rigid disc with a 10-mm diameter and ~1-mm thickness from 250 mg of RuO<sub>2</sub>. The RuO<sub>2</sub> powder compacted without the SPS current was very fragile and started to collapse soon after being immersed in H<sub>2</sub>SO<sub>4</sub> (aq) for the electrochemical measurement, thus requiring the electric current to solidify the RuO<sub>2</sub> powder. With an SPS current greater than 600 A, liquid seeped out of the disc, implying dehydration of the hydrous RuO<sub>2</sub> (see below about the water content).

The cyclic voltammograms of the SPS RuO<sub>2</sub> electrodes are shown in Fig. 2 by using the differential capacitance as the ordinate:

$$\frac{dQ}{dE} = \frac{I(E)/m}{|dE/dt|}$$

where  $Q$  is the electric charge,  $E$  is the potential,  $I$  is the voltammetric current,  $m$  is the mass of the SPS RuO<sub>2</sub> electrode and  $dE/dt$  is the CV scan rate. At the CV scan rate of 1 mV s<sup>-1</sup>, with the increasing SPS current, the magnitude of the differential capacitance decreased, and the asymmetry between the anodic and cathodic chargings diminished. At the CV scan rate of 20 mV s<sup>-1</sup>, for the RuO<sub>2</sub> electrodes prepared with the lower SPS currents, a resistive characteristic dominates the CV, whereas the electrodes prepared at the 1 kA SPS current retain their rectangular CV shape.

Fig. 3(a) shows the SPS current dependence of the total (integrated) capacitance  $C$  at the CV scan rate of 1 mV s<sup>-1</sup> defined as the average of the anodic and cathodic capacitances, i.e.,

$$C = \frac{1}{2m \{E(t_b) - E(t_a)\}} \int_{t_a}^{t_b} |I(t)| dt$$

where  $t_a$  and  $t_b$  are the time when the polarization was inverted; i.e.,  $I = 0$  at  $t = t_a$  and  $t = t_b$ . The gross capacitances of the SPS RuO<sub>2</sub> electrodes prepared at the SPS currents of 50–380 A are almost invariable at around 650 F g<sup>-1</sup> with the maximum of 708 F g<sup>-1</sup> at the SPS current of 380 A. This value coincides with the net capacitance of the electrode prepared by the conventional method in the present study (RuO<sub>2</sub>/10% PVdF 631 F g<sup>-1</sup> and RuO<sub>2</sub>/5% PVdF

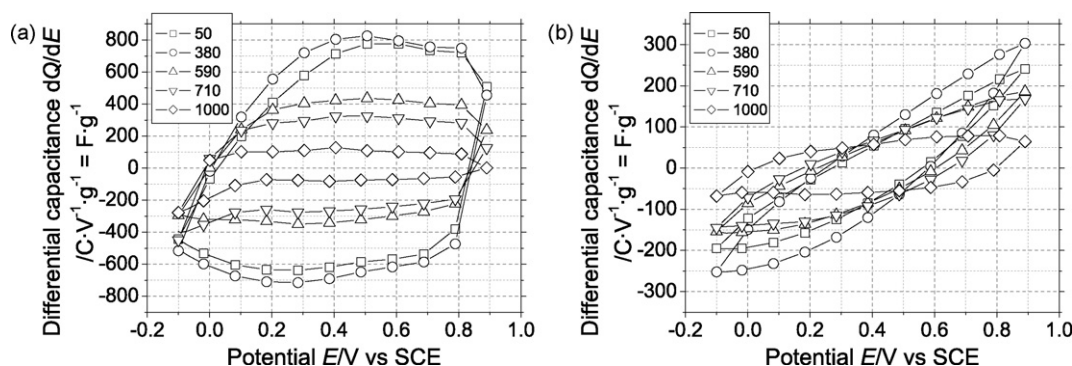


**Fig. 2.** Cyclic voltammograms of the RuO<sub>2</sub> electrodes compacted by the spark plasma sintering technique. The scan rates are (a) 1 mV s<sup>-1</sup> and (b) 20 mV s<sup>-1</sup>. Values in the figure legend are the SPS currents in A.

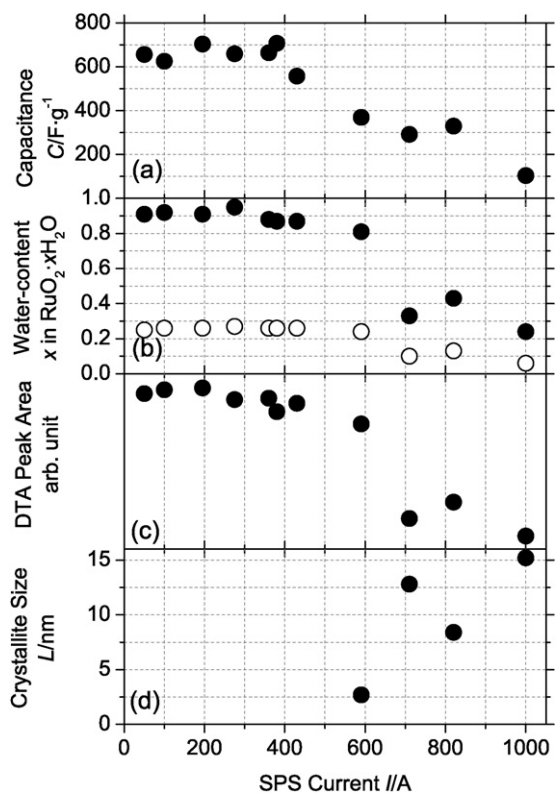


**Fig. 3.** (a) Specific capacitance at  $1 \text{ mV s}^{-1}$  CV scan rate, (b) water content (filled circles: total water, open circles: water desorbs at  $> 570 \text{ K}$ ), (c) DTA peak area of crystallization and (d) crystallite size as a function of the SPS current.

$636 \text{ F g}^{-1}$ ) and that reported by Zheng and Jow ( $720 \text{ F g}^{-1}$ ) [2]. By taking into account the mass of the binder in these electrodes, their gross capacitances were calculated to be 571, 598 and  $684 \text{ F g}^{-1}$ , respectively. That is, the SPS technique has the potential to improve the gravimetric capacitance of the  $\text{RuO}_2$  electrode by reducing the amount of binder without impairing the intrinsic capacitance of the material.

A further increase in the SPS current to greater than 400 A resulted in a gradual drop in the capacitance to  $100 \text{ F g}^{-1}$  at 1 kA. It is well known that the decrease in the capacitance of the  $\text{RuO}_2$  results from the loss of the hydrous amorphous state caused by annealing the ruthenium precursor at an elevated temperature [2,3,10–13]. Fig. 3(a) apparently suggests that the SPS current influences the material properties in a manner similar to the annealing temperature.

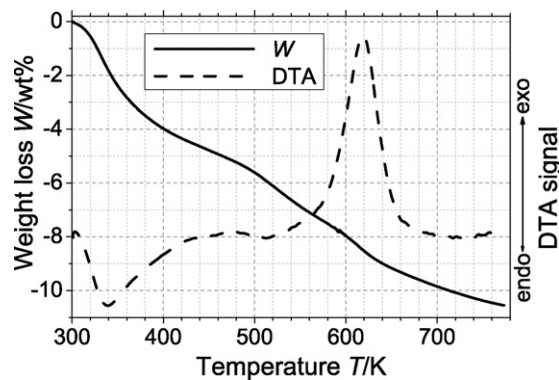


**Fig. 5.** TG–DTA analysis of  $\text{RuO}_2$  compacted at the SPS current of 380 A. The baseline is subtracted from the DTA signal.

The XRD measurement revealed that, while the materials electrified with less than 430 A retain their amorphous structure, the crystalline component starts to grow with the SPS current of more than 590 A as indicated in Fig. 3(d) which shows the crystallite size calculated from the width of the diffraction peak at  $2\theta = 28^\circ$  ( $[110]$  plane) based on Scherrer's equation.

Regardless of the SPS current from 0 to 1 kA, the BET surface area of the SPS  $\text{RuO}_2$  ranges between 50 and  $60 \text{ m}^2 \text{ g}^{-1}$ , showing no shift from the surface area of the starting  $\text{RuO}_2$  powder dried at 423 K. Similarly, we observed by SEM no distinctive SPS current dependence of the particle morphology. Fig. 4 shows the SEM images of the SPS  $\text{RuO}_2$  compacted at 380 A as a representative sample. The SPS  $\text{RuO}_2$  is an aggregate of 1–10  $\mu\text{m}$  particles, of which the surface has 10–20 nm of mesopores suggested by the  $\text{N}_2$  adsorption isotherm. The growth in the crystallite size observed by XRD must be taking place within the particles as they do not coalesce with each other within 1 s during the SPS electrification. This feature differentiates the effect of the SPS current from that of the long-period annealing which enlarges the particles as indicated by the decrease in the surface area of the  $\text{RuO}_2$  to less than half when the annealing temperature was raised from 423 to 673 K [3].

Fig. 5 shows the TG and DTA signals of the sample compacted at the SPS current of 380 A. The total water content (filled circles in Fig. 3(b)) was calculated from the total weight loss by heating the sample to 773 K based on the assumption that the total weight loss is due to the loss of  $\text{H}_2\text{O}$  only. Following the endothermic effect of dehydration at around 340 K, the exothermic effect of crystallization was observed around 620 K in the DTA signal. The open circles in Fig. 3(b) indicate the amount of water desorbing at higher than 570 K, which is approximately the on-set temperature of the

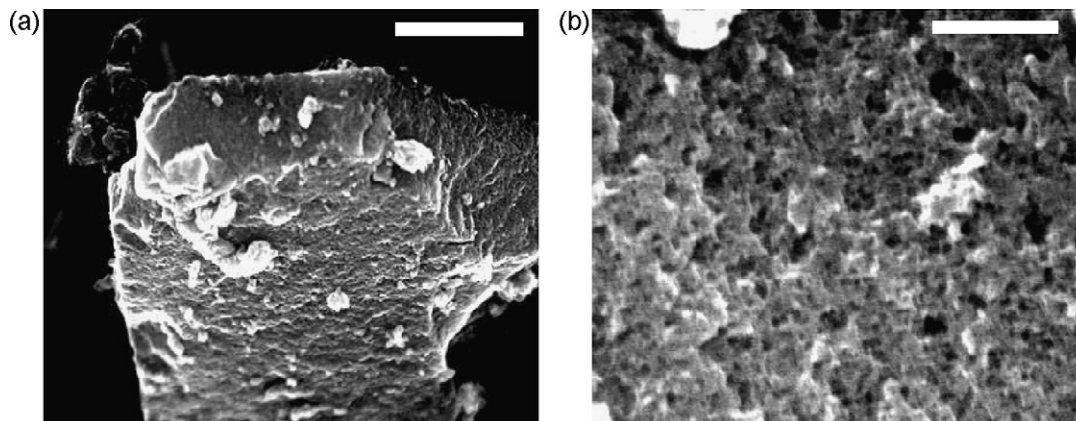


**Fig. 4.** SEM images of  $\text{RuO}_2$  molded at the SPS current of 380 A. Scale bars indicate (a) 1  $\mu\text{m}$  and (b) 100 nm.

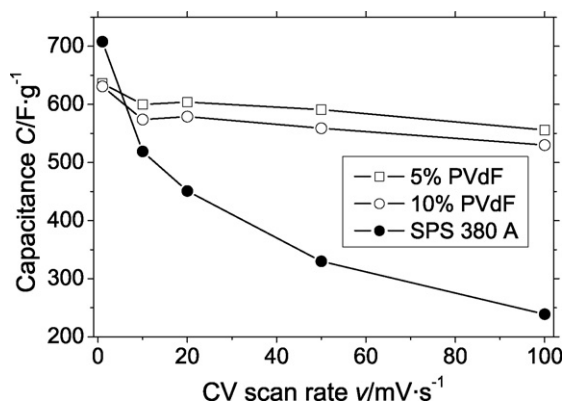


Fig. 6. Net capacitance  $C$  as a function of the CV scan rate  $v$ .

crystallization shown in the DTA. This trend in the water content roughly agrees with that reported in Ref. [13] in which the amount of tightly bound water was determined by X-ray photoelectron spectroscopy with respect to the annealing temperature of  $\text{RuO}_2$ . Although the quantitiveness of the heat flow is not guaranteed for the DTA in principle, it is reasonable in the present case to assume that the DTA peak area of the crystallization is roughly proportional to the fraction of the amorphous component remaining in the sample as long as we compare the peak area of the fixed mass (20 mg) of the same substance ( $\text{RuO}_2$ ) at the same temperature (620 K). Concomitant to the decrease in the capacitance and water content, the amorphous component in the SPS  $\text{RuO}_2$  electrode decreases with the increasing SPS current. These results suggest that the SPS current has an effect on the material properties in a manner similar to the annealing temperature, except that a short SPS current can solidify the powders before they grow. Under the present experimental conditions, the SPS current of 400 A

corresponds to the annealing temperature of 470 K at which the abrupt dehydration and crystallization take place in the hydrous amorphous  $\text{RuO}_2$  [3,13].

The rate performance of the SPS  $\text{RuO}_2$  electrode compacted at a 380 A SPS current is compared with the  $\text{RuO}_2$  electrodes prepared with the binder ( $\text{RuO}_2/5\%$  PVdF and  $\text{RuO}_2/10\%$  PVdF) in Fig. 6. Although at the CV scan rate of  $1 \text{ mV}\cdot\text{s}^{-1}$ , the SPS  $\text{RuO}_2$  electrode has a greater capacitance than  $\text{RuO}_2/\text{PVdF}$ , it is soon surpassed at the higher CV scan rate.

Based on the results described above, certain trials to improve the performance of the SPS  $\text{RuO}_2$  electrode are currently underway, such as adding a conductive agent to enhance the electron conductivity, though at the cost of the gravimetric capacitance, investigating the particle adhesion by varying the particle size, preparing thinner electrodes, etc.

## References

- [1] S. Trasatti, G. Buzzanca, *J. Electroanal. Chem.* 29 (1971) A1–A5.
- [2] J.P. Zheng, T.R. Jow, *J. Electrochem. Soc.* 142 (1) (1995) L6–L9.
- [3] J.P. Zheng, P.J. Cygan, T.R. Jow, *J. Electrochem. Soc.* 142 (8) (1995) 2699–2703.
- [4] V. Srinivasan, J.W. Weidner, *J. Electrochem. Soc.* 144 (8) (1997) L210–L213.
- [5] N. Miura, S. Oonishi, K.R. Prasad, *Electrochem. Solid-State Lett.* 7 (8) (2004) A247–A249.
- [6] V. Subramanian, H. Zhu, R. Vajtai, P.M. Ajayan, B. Wei, *J. Phys. Chem. B* 109 (2005) 20207–20214.
- [7] O. Barbieri, M. Hahn, A. Foelske, R. Kötz, *J. Electrochem. Soc.* 153 (2006) A2049–A2054.
- [8] M. Tokita, *J. Soc. Powder Technol. Jpn.* 30 (1993) 790–804.
- [9] Z.A. Munir, U. Anselmi-Tamburini, M. Ohyanagi, *J. Mater. Sci.* 41 (2006) 763–777.
- [10] H. Kim, B.N. Popov, *J. Power Sources* 104 (2002) 52–61.
- [11] W. Dmowski, T. Egami, K.E. Swider-Lyons, C.T. Love, D.R. Rolison, *J. Phys. Chem. B* 106 (2002) 12677–12683.
- [12] W. Sugimoto, H. Iwata, K. Yokoshima, Y. Murakami, Y. Takasu, *J. Phys. Chem. B* 109 (2005) 7330–7338.
- [13] A. Foelske, O. Barbieri, M. Hahn, R. Kötz, *Electrochem. Solid-State Lett.* 9 (2006) A268–A272.